

Commercialization of Quantum Well Infrared Photodetector QWIP™ Focal Plane Arrays

C. A. Kukkonen, S. D. Gunapala*, S. V. Bandara*, and J. K. Liu*, J. Llorens

QWIP Technologies, a ViaSpace Company, 2400 Lincoln Avenue, Altadena, CA 91001

* Center for Space Microelectronics Technology, Jet Propulsion Laboratory,
California Institute of Technology, Pasadena, CA 91109

ABSTRACT

Many commercial and government applications need high performance, large format, long-wavelength infrared (LWIR) detector arrays in the range of 6-20 μm . NASA and the Ballistic Missile Defense Organization (BMDO) have devoted a significant effort to develop highly sensitive infrared (IR) detectors and large format focal plane arrays (FPAs) based on novel, "artificial", low effective band-gap semiconductor material systems such as GaAs/AlGaAs. Caltech's Jet Propulsion Laboratory (JPL) under contract from NASA and BMDO has extensively pursued GaAs/AlGaAs based multi-quantum wells (MQWs) for IR radiation detection. Optimization of the detector design, light coupling schemes, large format focal plane array fabrication and packaging have culminated in the realization of portable infrared cameras with a mid-format (256 x 256 pixel) FPA of QWIP detectors and the demonstration of a TV format (i.e., 640 x 486) QWIP camera. QWIP Technologies under an agreement with Caltech is manufacturing the QWIP-Chip™, a 320 x 256 element FPA, which will be available in the summer of 1999. In this paper we discuss the advantages of MQW technology and our experience in the commercialization of QWIP™ FPAs.

1. INTRODUCTION

Visible light spanning the wavelength range from blue ($\sim 0.4 \mu\text{m}$) to red ($\sim 0.7 \mu\text{m}$) is a tiny slice of the electromagnetic spectrum. While an enormous wealth of scientific information can be and is obtained through imaging and spectroscopy of objects in visible light, the invisible portion of the spectrum can be harvested to yield both more detailed and new information. Objects that are invisible to the human eye may be visible at other wavelengths. For instance, an object at room temperature ($\sim 300 \text{ K}$) and in complete darkness may be perfectly invisible to the human eye; but its temperature will make it glow in the infrared (at wavelengths longer than the $0.7 \mu\text{m}$ wavelength), shining brightest at an infrared (IR) wavelength of $8.5 \mu\text{m}$. A camera which can see $8.5 \mu\text{m}$ light and convert this IR image into a visible image on a standard TV monitor or camcorder viewfinder may make the invisible scene spring to life. Temperature and emissivity variations in the IR scene translate to contrast or color variations in the visible image, revealing objects and their motion. This is the basis of a night-vision (or IR) camera.

While the invisible portion of the electromagnetic spectrum includes gamma rays, X rays, and ultraviolet rays beyond the blue end of the visible spectrum, and IR rays (spanning a wide wavelength swath from $\sim 0.7 \mu\text{m}$ to $\sim 1 \text{ mm}$) and microwaves beyond the red end, light detectors operating in the 3-18 μm wavelength range hold a special significance. Potential applications at these wavelengths range from the mundane to the sublime. As stated earlier, room temperature objects glow brightest in this wavelength range. Detectors with the sharpest eyes for light at these wavelengths are ideal for a variety of ground- and space-based applications such as night vision, early warning systems, navigation, flight control systems, weather monitoring, security and surveillance, medical imaging, etc. In addition, they can be used to monitor and measure pollution, relative humidity profiles, and the distribution of different gases (e.g., O_3 , CO , N_2O , etc.) in the atmosphere. This is due to the fact that most of the absorption lines of gas molecules lie in this IR spectral region. The Earth's atmosphere is opaque to most of the IR; of its few transparent windows, the 8-12 μm is one of the clearest. Cameras operating in this wavelength range and used in ground-based telescopes will be able to see through the Earth's atmosphere, image distant stars and galaxies (including those invisible to telescopes equipped with normal visible eyes), and help in the search for cold objects such as planets orbiting nearby stars. IR detectors operating in the 3-20 μm wavelength range thus find many applications in NASA, medicine, commerce, and defense^{1,2}.

Since the mid-fifties many government agencies such as NASA, Department of Defense (DoD), etc. have spent a very large amounts of money in the development of novel IR detectors. The most common photon detectors are based on the principle of interband absorption in narrow bandgap semiconductors like InSb, $\text{Hg}_x\text{Cd}_{1-x}\text{Te}$, etc. IR radiation is absorbed by the photosensitive material when an incoming photon has sufficient energy $E (= h\nu)$ to photoexcite an electron across the energy bandgap from the valence band to the conduction band. This process is equivalent to providing enough energy to free a valence electron (so called, because it is loosely bound to the atoms in the semiconductor crystal) and make it available for the conduction of electric current. Such a photoexcited electron is called a photoelectron. Photons with energies less than the bandgap energy are not absorbed; they simply pass through the semiconductor. The bandgap energy therefore defines the low energy (or long wavelength cut-off) absorption edge of the detector. Applying a voltage bias across the detector creates an electric field that sweeps out both photocarriers producing a photocurrent in the external circuit. Such a detector need not be doped and is called an intrinsic detector. Large two-dimensional arrays of InSb (512×512 pixels) and $\text{Hg}_{1-x}\text{Cd}_x\text{Te}$ (128×128 pixels) detectors have already been demonstrated up to cut-off wavelengths of $5 \mu\text{m}$ and $11 \mu\text{m}$ respectively. The move to larger pixel arrays is driven by the need for greater scene resolution. Since the bandgap of InSb is fixed, InSb photodetectors cannot detect light at wavelengths longer than $5 \mu\text{m}$.

Longer wavelengths can be accessed by narrowing the bandgap of $\text{Hg}_{1-x}\text{Cd}_x\text{Te}$ by changing its alloy composition x . However, such narrow bandgap materials are more difficult to grow and process into devices, reducing the yield and increasing the cost of the arrays³. These difficulties motivate the exploration of *artificial low effective* bandgap structures built from wide bandgap semiconductors such as GaAs (see Fig. 1) which are far easier to grow and process into devices. A low effective bandgap can be created in a quantum well, which resides entirely in either the conduction band or the valence band of a wide bandgap semiconductor like GaAs. Such a GaAs-based Quantum Well Infrared Photodetector (QWIP) then benefits from the highly mature GaAs growth and processing technologies, a benefit that becomes increasingly critical at the longer wavelengths where narrow bandgap materials become more difficult to work with. As a result, in 1991 Jet Propulsion Laboratory (JPL) started to investigate GaAs/AlGaAs based MQW structures for IR radiation detection.

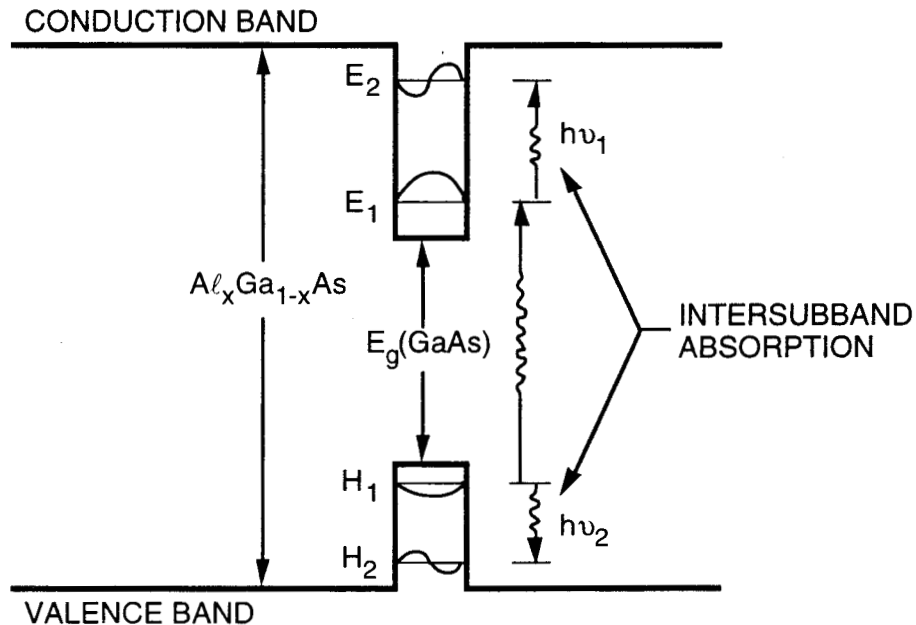


Figure 1. Schematic band diagram of a quantum well. Intersubband absorption can take place between the energy levels of a quantum well associated with the conduction band or the valence band.

As a consequence, JPL has demonstrated the first hand-held and palm-size 256×256 LWIR imaging cameras, and a TV format (i.e., 640×486) LWIR imaging camera based on GaAs/AlGaAs MQW structures. Broad-band, dualband, and high-performance QWIPs for NASA's astronomy and DoD's strategic applications have also been demonstrated, and have resulted in the introduction of QWIPTM sensor products by QWIP Technologies..

2. QUANTUM WELL INFRARED PHOTODETECTORS (QWIPs)

The idea of using a quantum well to detect light can be understood by the basic principles of quantum mechanics⁴. An electron in a square quantum well is the classic particle-in-a-box of basic quantum mechanics. Such a square quantum well can be created in the lattice-matched GaAs/Al_xGa_{1-x}As material system by sandwiching a layer of GaAs between two layers of Al_xGa_{1-x}As. The bandgap of Al_xGa_{1-x}As being larger than that of GaAs, results in a square quantum well for electrons in the conduction band: the GaAs layer is the well layer; the Al_xGa_{1-x}As layers on either side are the potential barriers. The depth of the potential well (= the height of the potential barrier) can be precisely controlled by controlling the Al mole fraction x in the Al_xGa_{1-x}As barrier layers. State-of-the-art crystal growth techniques like molecular beam epitaxy (MBE) permit the epitaxial growth of such layers, typically on a 3-6 inch diameter ~600- μ m thick GaAs substrate, with ultra-high purity and with control of layer thickness down to a fraction of a molecular layer. This allows the width of the GaAs well layer (one of the design parameters) to be precisely controlled, and the interfaces between the well and barrier layers to be made truly sharp to produce a textbook square quantum well. A controlled number of ground state electrons are provided by doping the GaAs well with Si (an n-type dopant) during the MBE growth. Several quantum wells (sandwiched between barriers) are usually grown stacked on top of each other to increase photon absorption. The upper limit on this number for a typical detector structure in this material system is around 50, about the number of wells and barriers that a photoelectron can traverse in an electric field without being captured by a well downstream from the well which the electron originated. The entire MQW stack is sandwiched between heavily-doped top (called the emitter) and bottom (called the collector) GaAs layers which provide electrical contacts to the device. Absorption of a photon excites an electron from the ground state to the first excited state near the well top, where it can tunnel out to the continuum (continuous energy levels above the quantum well) in the presence of an external voltage bias, thereby producing a photocurrent as shown in Fig. 2.

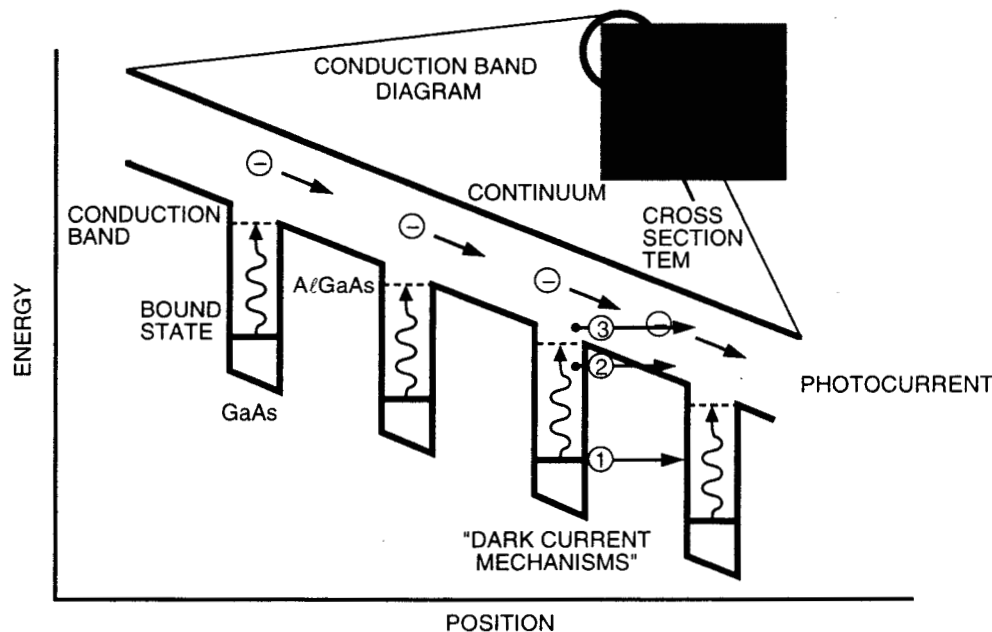


Figure 2 A typical conduction-band diagram of very long wavelength bound-to-continuum quantum well infrared photodetector.

3. DARK CURRENT REDUCTION

In addition to the photocurrent, all detectors including QWIPs produce a parasitic current called dark current, which must be minimized to achieve high performance. The dark current is the current flowing through the detector when it is in the dark (i.e. with no photons impinging on it) and is ideally zero. In most applications the *total* current flowing through the detector is measured and there is no way to distinguish the dark current from the photocurrent. Though this dark current can be approximately subtracted in the image-processing electronics, a high dark current implies that the detector blinds itself even when it sees no photons. When it does see photons the image-processing electronics are swamped by the dark electrons with very little capacity left to process the photoelectrons. In QWIPs, the dark current originates from three different mechanisms, as shown in Fig. 2. The dark current arising from the first process is due to quantum mechanical tunneling of ground state electrons from well to well through the Al_xGa_{1-x}As barriers (sequential tunneling). This process is independent of

temperature. Sequential tunneling dominates the dark current at very low temperatures (<30 K). The second mechanism is thermally-assisted tunneling which involves thermal excitation of a ground state electron followed by its tunneling through the narrower tip of the barrier into the continuum energy levels. This process governs the dark current at medium temperatures. The third mechanism is classical thermionic emission (the emission of electrons over a finite potential barrier due to their finite temperature) and dominates the dark current at higher temperatures (>45 K). Reducing the dark current due to this mechanism is critical to the success of the QWIP since it enables the highly desirable higher temperature camera operation.

A method to reduce the dark current due to thermionic emission and optimize the performance of LWIR MQW's has been devised by Sarath Gunapala *et al.*⁴ at JPL. This QWIP uses *bound-to-quasibound* intersubband absorption (occurring when the first excited state is in resonance with the top of the well). This transition maximizes the intersubband absorption while maintaining excellent electron transport. The major advantage of this design lies in the fact that it increases the energy barrier to thermionic emission compared to the case of the bound-to-continuum structure (see Fig. 3), and results in the substantial performance advantage of the QWIP-Chip™ FPA.

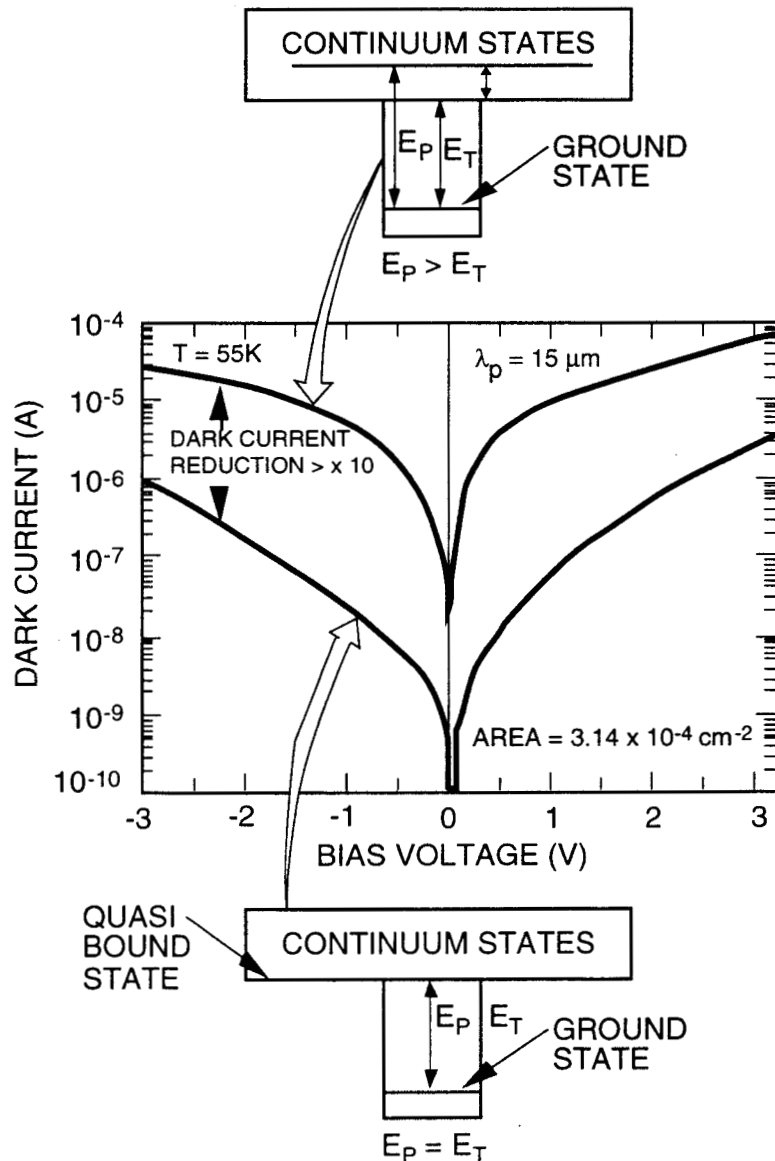


Figure 3. Comparison of dark currents of bound-to-continuum and bound-to-quasibound LWIR QWIPs as a function of bias voltage at temperature $T = 70 K$. Data were taken with a $200 \mu m$ diam test structure and normalized to $28 \times 28 \mu m^2$ pixel.

4. LIGHT COUPLING SCHEMES FOR QWIPs

In order to be absorbed by the electrons in the quantum wells, the incoming light must have an electric field component in the quantum well direction (i.e., in the growth direction, normal to the layers). Only in this situation is the electric field of the light coupled to the quantized electron momentum, enabling a photon to excite an electron and get absorbed in the process. Light being a transverse wave (whose electric field is perpendicular to the direction of travel). This quantum mechanical selection rule means that light striking the layers normally (the most direct way to illuminate an imaging array of detectors) is not absorbed. This clearly limits the configuration of detectors to linear arrays and single elements. For imaging, it is necessary to be able to couple light uniformly to two-dimensional arrays of detectors.

This is accomplished by putting a special reflector on the detector top and illuminating the detector from the back. To be useful, the mirror has to be rough (on the scale of the wavelength of the light in the detector's GaAs material). This roughness may be either periodic or random (see Fig. 4). A rough mirror scatters or sprays the incident light back in a cone (i.e., the roughness ensures that the angle of reflection no longer equals the angle of incidence). The details of the cone depend on the details of the roughness. This cone now strikes the bottom side. Those rays that are within a critical angle of the normal (17° for the GaAs-air interface) refract and escape back into the air. The rest suffer total internal reflection with the back surface acting as a smooth mirror. The internally reflected rays are once again reflected off the top rough mirror. What happens next depends on whether the roughness of the

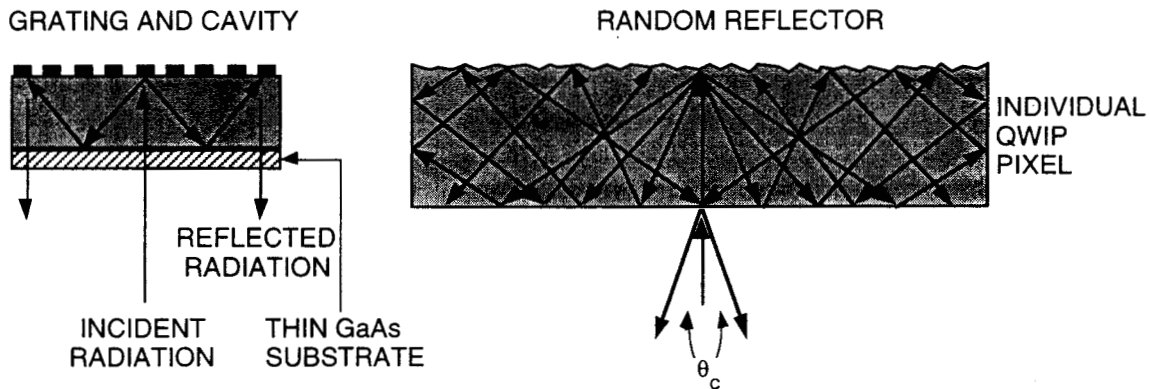


Figure 4. (a) Schematic side view of a 2-D periodic grating coupled QWIP pixel. A thinned pixel (or substrate removed) will get two light absorbing passes before it leaves the pixel. (b) Schematic side view of a thin QWIP pixel with a random reflector.

top mirror is periodic or random. If it is periodic, the top mirror will scatter or bend these rays so that they are all normal to the quantum well layers again. These rays pass through the detector and out of the backside (see Fig. 4). A randomly roughened mirror, on the other hand, will randomly reflect or scatter all the rays internally reflected on to it from the bottom side each time, thereby allowing the incident light to bounce back and forth between the detector top and back surfaces several times. Only light within a 17° (from normal) cone escapes out of the backside. Clever design can reduce the amount of light in the escape cone but cannot eliminate it altogether. For instance, if the random reflector is designed with two levels of rough surfaces having the same areas but located a quarter wavelength ($\lambda_{\text{GaAs}}/4$) apart, the normally reflected light intensities from the top and bottom surfaces of the reflector are equal and 180° out of phase (see Fig. 4). This maximizes the destructive interference at normal reflection and lowers light leakage through the escape cone. Both light coupling schemes are fabricated on the MQW structures using standard photolithography and CCl_2F_2 selective dry etching.

5. DEVELOPMENT OF QWIP IMAGING ARRAYS

(A) 256 x 256 Hand-held LWIR Imaging Camera

The first 256 x 256 LWIR hand-held imaging camera was demonstrated by Gunapala *et al*⁶. The device structure of this FPA consisted of a bound-to-quasibound QWIP containing 50 periods of a 45 Å well of GaAs (doped $n = 4 \times 10^{17} \text{ cm}^{-3}$) and a 500 Å barrier of $\text{Al}_{0.3}\text{Ga}_{0.7}\text{As}$. After the random reflector array was defined by the lithography and dry etching, the photoconductive pixels of the 256 x 256 FPAs were fabricated by wet chemical etching through the photosensitive GaAs/ $\text{Al}_x\text{Ga}_{1-x}\text{As}$ MQW layers into the 0.5 μm thick doped GaAs bottom contact layer. The pitch of the FPA is 38 μm and the actual pixel size is 28 x 28 μm². The random reflectors on top of the detectors were then covered with Au/Ge and Au for

Ohmic contact and reflection. A single FPA was chosen and hybridized (via indium bump-bonding process) to a 256 x 256 CMOS readout multiplexer (Amber AE-166) and biased at $V_B = -1.0$ V. The FPA was back-illuminated through the flat thinned substrate membrane (thickness ~ 1300 Å). This initial array gave excellent images with 99.98% of the pixels working (number of dead pixels ~ 10), demonstrating the high operability of GaAs technology. The measured NE ΔT of the FPA at an operating temperature of $T = 70$ K, bias $V_B = -1$ V, and for 300 K background is 15 mK. This agrees reasonably with our estimated value of 8 mK based on test structure data. The peak quantum efficiency of the FPA was 3.3% (lower FPA quantum efficiency is attributed to 54% fill factor and 90% charge injection efficiency) and this corresponds to an average of three passes of infrared radiation (equivalent to a single 45° pass) through the photosensitive MQW region.

A 256 x 256 QWIP hybrid was mounted onto a 250 mW integral Sterling closed-cycle cooler assembly and installed into an Amber RADIANCE 1™ camera-body to demonstrate the hand-held LWIR camera (shown in Fig. 5). The camera is equipped with a 32-bit floating-point digital signal processor combined with multi-tasking software, providing the speed and power to execute complex image-processing and analysis functions inside the camera body itself. The other element of the camera is a 100 mm focal length germanium lens, with a 5.5 degree field of view. It is designed to be transparent in the 8-12 μm wavelength range to be compatible with the QWIP's 8.5 μm operation.

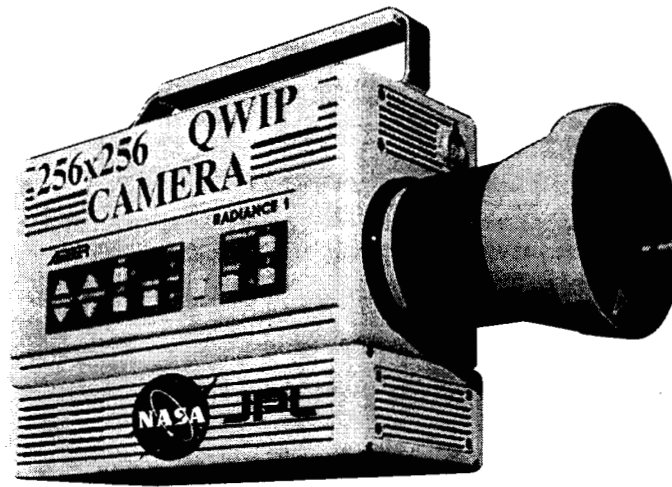


Figure 5. Picture of the first 256 x 256 hand-held long wavelength QWIP camera (QWIP RADIANCE).

(B) 640 x 486 LWIR Imaging Camera

After the 2-D grating array was defined by the photolithography and dry etching, the photoconductive pixels of the 640 x 486 FPAs were fabricated⁷ by wet chemical etching through the photosensitive GaAs/Al_xGa_{1-x}As MQW layers into the 0.5 μm thick doped GaAs bottom contact layer. The pitch of the FPA is 25 μm and the actual pixel size is 18 x 18 μm^2 . The cross gratings on top of the detectors were then covered with Au/Ge and Au for Ohmic contact and reflection. A single QWIP detector array was chosen and hybridized to a 640 x 486 direct injection silicon readout multiplexer (Amber AE-181) and biased at $V_B = -2.0$ V. The FPA was back-illuminated through the flat thinned substrate membrane (thickness ~ 1300 Å). This thinned GaAs detector array membrane has completely eliminated the thermal mismatch between the silicon CMOS readout multiplexer and the GaAs based QWIP detector array. Basically, the thinned GaAs based QWIP detector array membrane adapts to the thermal expansion and contraction coefficients of the silicon readout multiplexer. Therefore, this thinning has played an extremely important role in the fabrication of large area highly reliable FPA hybrids that will survive extensive thermal cycling. In addition, this thinning has completely eliminated the pixel-to-pixel optical cross-talk of the FPA. This initial array gave excellent images with 99.9% of the pixels working, demonstrating the high operability of GaAs technology. The experimentally measured NE ΔT of the FPA is 36 mK at an operating temperature of $T = 70$ K, bias $V_B = -2$ V, and at 300 K background. This agrees reasonably with our estimated value of 25 mK based on test structure data. The experimentally measured peak quantum efficiency of the FPA was 2.3% (lower focal plane array quantum efficiency is attributed to 51% fill factor and 30% reflection loss from the GaAs back surface). Thus, the corrected quantum efficiency of focal plane detectors is 6.5% and this corresponds to an average of two passes of IR radiation (equivalent to a single 45° pass) through the photosensitive MQW region.

A 640 x 486 QWIP FPA hybrid was mounted onto a 84-pin lead-less chip carrier and installed into a laboratory dewar which is cooled by liquid nitrogen (to demonstrate a LWIR imaging camera). The other element of the camera is a 100 mm focal length AR coated germanium lens, which gives a $9.2^\circ \times 6.9^\circ$ field of view. The uncorrected NE Δ T non-uniformity of the 640 x 486 FPA is about 5.6% (= sigma/ mean).



Figure 6. This picture was taken in the night (around midnight) and it clearly shows where automobiles were parked during the day time. This image demonstrates the high sensitivity of the 640 x 486 long-wavelength QWIP staring array camera.

Video images were taken at a frame rate of 30 Hz at temperatures as high as $T = 70$ K using a ROC capacitor having a charge capacity of 9×10^6 electrons. The non-uniformity after two-point (17° and 27° Celsius) correction improves to an impressive 0.1%. Figure 6 shows a frame of a video image taken with this long-wavelength 640 x 486 QWIP camera. This image demonstrates the high sensitivity of the 640 x 486 long-wavelength QWIP staring array camera. As mentioned earlier, this high operability is due to the excellent GaAs growth uniformity and the mature GaAs processing technology.

6. COMMERCIALIZATION

These results clearly show QWIP FPAs are very sensitive and manufacturable. QWIP Technologies, a Via Space Company under agreement with Caltech is manufacturing the QWIP-ChipTM, a 320 x 256 format QWIPTM FPA. The first product will be spectrally centered at $8.5 \mu\text{m}$ (see Fig. 7) with $30 \mu\text{m}$ pitch and will be available in August of this year in low rate initial quantities of 20 per month to the end of the year. Production will ramp up to 100 QWIPTM FPAs per month beginning in January of year 2000. Initially, 3-inch GaAs wafers will be used until late this year when the switch will be made to 4-inch GaAs wafers. Current limitations in uniformity of MBE grown QWIP structures over large areas will limit production material to 4-inch diameter GaAs wafers at least through year 2000. The Indigo Systems 9705 windowing readout, with snapshot mode capability, will be used in this first product. Early in the second quarter of year 2000 the second product will begin low rate initial production ramping up to full scale late in the third quarter. This second product will be a 640 x 512 QWIP-ChipTM QWIP FPA.

Detector Type	QWIP (Quantum Well Infrared Photodetector)
Multiplexer Type	Direct Injection
Integration Mode	Snapshot (flexible integration mode)
Windowing	Yes (dynamic windowing)
Array Size	320 x 256 ¹
Pixel Size (pitch)	30 microns x 30 microns
Fill Factor	>85%
Spectral Response	8-9 microns ¹
Spectral Band Center	8.5 microns
Mean Temporal NE Δ T (@ f/2 optics, 300 K background temperature, 15 msec integration time)	35 mK @ 75 K, 30 mK @ 70 K 25 mK @ 65 K, 20 mK @ 60 K
Operating Temperature	20-80 K
Operability	>99.9%
Full Scale Uncorrected Nonuniformity (s/m)	<5%
D _{BB} * (@ f/2 optics, 300 K background temperature, 15 msec integration time)	2.0E10 @ 75 K, 3.2E10 @ 70 K, 3.8E10 @ 65 K 4.0E10 @ 60 K
Radiation Hardness	Yes (1.6 MR)
Charge Storage Capacity	1.8E07 electrons
Max Frame Rate	Full frame: 100 Hz single output, 400 Hz with 4 outputs (higher speeds possible with smaller frames)
Number of Outputs	1, 2, or 4
Integration Time	Variable
Max Data Rate	10 MHz per channel
Total Crosstalk	Negligible
Required Clocks	4
Required Biases	3
Power Dissipation	<20 mW @ 60 Hz frame rate (single output)
Readout Noise	<500 electrons

¹Standard product. Custom detectors available from 2.7 to 28 microns. Larger or smaller formats also available
*Specifications subject to change without notice.

Figure 7. QWIP-Chip™ preliminary specifications.

QWIP detector process methodology developed at JPL is being transitioned to the manufacturing environment which utilize high volume process technology developed for III-V materials for cellular communication industry. Analysis of the process flow from raw materials to hybridized FPA has helped to identify the yield and schedule drivers and resulted in a manufacturing plan which at the current time calls for outsourcing of a significant portion of the build process. The company plans to bring the necessary capabilities in house within the next two years. QWIP Technologies also plans to diversify its product line to include sensor engines and imaging systems over next several years.

7. SUMMARY

In recent years, an exceptionally rapid progress has been made in the development of long-wavelength QWIP™ FPAs. It is now possible for QWIPs to achieve excellent performance (e.g., FPA blackbody detectivities as high as D_{BB}* ~3.2 x 10¹⁰ cmvHz/W at 70 K for 8-9 μm) and be fabricated into large inexpensive low-noise imaging arrays. A 70 K operating temperature can be easily achieved by single-stage Stirling cycle coolers, which allowed us to demonstrate the first palm-size 256 x 256 FPA LWIR camera based on QWIPs. Weighing about 2.5 pounds, the QWIP InfraCam is entirely self-contained, with no extra boxes for control, cooling, or image processing. Its sharp, inexpensive, large, uniform, infrared eye (which can be tailored to see a particular IR wavelength) makes the QWIP palm-size camera a cost-effective new tool for imaging and spectroscopy applications. QWIP Technologies, a Via Space Company is already manufacturing the QWIP-Chip™, a 9 μm cutoff 320 x 256 element QWIP™ FPA, which will be available in the summer of 1999. A 640 x 512 element FPA is planned for the year 2000.

8. ACKNOWLEDGMENTS

The research described in this paper was performed by the Center for Space Microelectronics Technology, Jet Propulsion Laboratory, California Institute of Technology, and was jointly sponsored by the National Aeronautics and Space Administration Office of Space Science, the Ballistic Missile Defense Organization / Innovative Science & Technology Office.

9. REFERENCES

1. M. T. Chahine, Proceedings of Innovative Long Wavelength Infrared Detector Workshop, Pasadena, California, April 24-26, 1990.
2. Duston, "BMDO's IS&T faces new hi-tech priorities", *BMD Monitor*, pp 180-183, May 19, 1995.
3. F. Levine, *J. Appl. Phys.* **74**, R1 (1993).
4. D. Gunapala and K. M. S. V. Bandara, *Physics of Thin Films*, Academic Press, **21**, 113 (1995).
5. Sarath D. Gunapala, John K. Liu, Jin S. Park, Mani Sundaram, Craig A. Shott, Ted Hoelter, True-Lon Lin, S. T. Massie, Paul D. Maker, Richard E. Muller, and Gabby Sarusi "9 μm Cutoff 256 x 256 GaAs/Al_xGa_{1-x}As Quantum Well Infrared Photodetector Hand-Held Camera", *IEEE Trans. Electron Devices*, **44**, pp. 51-57, 1997.
6. Sarath D. Gunapala, Jin S. Park, Gabby Sarusi, True-Lon. Lin, John K. Liu, Paul D. Maker, Richard E. Muller, Craig A. Shott, and Ted Hoelter, "15 μm 128 x 128 GaAs/AlGaAs Quantum Well Infrared Photodetector Focal Plane Array Camera", *IEEE Trans. Electron Devices*, **44**, pp. 45-50, 1997.
7. Sarath D. Gunapala, Sumith V. Bandara, John K. Liu, Winn Hong, Mani Sundaram, Paul D. Maker, Richard E. Muller, Craig A. Shott, and Ronald Carralejo "Long-Wavelength 640 x 486 GaAs/Al_xGa_{1-x}As Quantum Well Infrared Photodetector Snap-shot Camera", *IEEE Trans. Electron Devices*, **45**, pp. 1890-1895, 1998.
8. V. Bandara, S. D. Gunapala, J. K. Liu, E. M. Mumolo, W. Hong, D. K. Sengupta, and M. J. McKelvey, *Appl. Phys. Lett.*, **72** 2427, 1998.
9. D. Gunapala, S. V. Bandara, J. K. Liu, W. Hong, E. M. Luong, J. M. Mumolo, M. J. McKelvey, D. K. Sengupta, A. Singh, C. A. Shott, R. Carralejo, P. D. Maker, J. J. Bock, M. E. Ressler, M. W. Werner, and T. N. Krabach, "Quantum Well Infrared Photodetectors Research and Development at Jet Propulsion Laboratory", *SPIE Proceeding, Infrared Detectors and Focal Plane Arrays V*, pp. 382-395, Vol. 3379, 1998.